IOPscience iopscience.iop.org

Home Search Collections Journals About Contact us My IOPscience

Magnetothermopower in silicon MOSFETs

This article has been downloaded from IOPscience. Please scroll down to see the full text article.

1993 J. Phys.: Condens. Matter 5 1355

(http://iopscience.iop.org/0953-8984/5/9/020)

View the table of contents for this issue, or go to the journal homepage for more

Download details:
IP Address: 171.66.16.159
The article was downloaded on 12/05/2010 at 13:00

Please note that terms and conditions apply.

J. Phys.: Condens. Matter 5 (1993) 1355–1364. Printed in the UK

# Magnetothermopower in silicon MOSFETS

G Qin†§, T M Fromhold†||, P N Butcher†, B G Mulimani†, J P Oxley‡ and B L Gallagher‡

† Department of Physics, University of Warwick, Coventry CV4 7AL, UK
‡ Department of Physics, University of Nottingham, Nottingham NG7 2RD, UK

Received 28 August 1992, in final form 7 December 1992

**Abstract.** The phonon drag and electronic diffusion contributions to the tensor **M** which determines the heat flux $U = \mathbf{M} \cdot E$ is calculated for a two-dimensional electron gas in a perpendicular magnetic field $B$. The drag component is obtained using Boltzmann transport and diffusion is included using the lowest-order cumulant approximation to describe scattering between Landau states with different orbit centres. The 2D Landau levels have Gaussian model lineshapes with RMS width $\gamma = CB^{1/2}$ which is the only adjustable parameter. At temperature $T = 5.02$ K, drag dominates the predicted $M_{yx}(B)$ values which are in good agreement with new data for Si MOSFETs taking $C = 0.6$ meV $\mathrm{T}^{-1/2}$. The calculated $M_{xx}$ values are in worse accord with the data because the predicted drag contribution $M^{\mathrm{g}}_{xx}$ is zero. Both $M_{xx}$ and $M_{yx}$ reveal magneto-oscillations originating from fluctuations in the density of states at the Fermi level. We show that at $T = 5.02$ K, setting $M^{\mathrm{g}}_{xx} = 0$ has little effect on the accuracy of the magnetothermopower $S_{xx}(B)$ but yields poor approximations to the off-diagonal term $S_{yx}(B)$. At $T = 1.47$ K, these thermopower components are diffusion-dominated. The predicted values are comparable to experiment although the magneto-oscillations are overemphasized in $S_{yx}$ and underestimated in $S_{xx}$.

## 1. Introduction

A quantizing magnetic induction field $B||z$, perpendicular to the plane of a two-dimensional electron gas (2DEG) produces strong modulation of the electronic density of states. This has pronounced effects on the components of the magnetothermopower tensor $\mathbf{S}(B)$ which exhibit oscillatory behaviour, reflecting the field dependence of the density of states $D(E_{\mathrm{F}})$ at the Fermi energy [1,2].

In GaAs/(AlGa)As heterostructures the phonon drag contribution dominates the magnetothermopower for temperatures $T$ in the range 1–10 K [1–4]. By contrast, stronger screening of the electron–phonon interaction in Si MOSFETs suppresses the phonon drag by approximately three orders of magnitude so that electronic diffusion dominates the thermopower for $T < 2$ K [5,6]. We present new measurements of the magnetothermopower in Si MOSFETs at $T = 1.47$ K (diffusion-dominated) and at $T = 5.02$ K (drag-dominated). Results for intermediate temperatures are given by Oxley *et al* [6].

§ Present address: Department of Physics, Nanjing University, Nanjing 210008, People's Republic of China.

|| Present address: Department of Physics, University of Nottingham, Nottingham NG7 2RD, UK.

We have generalized the theory of phonon drag magnetothermopower in GaAs/(AlGa)As structures developed by Kubakaddi [1], Lyo [2] and Fromhold *et al* [4,7] to the case of Si MOSFETs. We show that at $T = 5.02$ K, the values of $-S_{xx}$ predicted by this theory are in good agreement with experiment. By contrast, the observed $S_{yx}$ values are poorly accounted for. This discrepancy has also been reported in GaAs/(AlGa)As structures by Fromhold *et al* [4].

In section 2 we describe a theory for the diffusion magnetothermopower of Si MOSFETs. The model is based on Gerhardts' lowest-order cumulant approximation to the energy-dependent electrical conductivity tensors $\sigma_{xx}(E)$ and $\sigma_{yx}(E)$ [10] and assumes a Gaussian lineshape for the Landau levels. The diffusion calculations yield the correct magnitude of the magnetothermopower at $T = 1.47$ K but give a poor account of the observed magneto-oscillatory amplitudes.

## 2. A model for the phonon drag and electronic diffusion magnetothermopower

Consider a magnetic induction field $B = (0,0,B)$ parallel to the $\langle 100 \rangle$ growth direction and normal to the plane of a 2DEG in a Si MOSFET. Isotropy in the $x$–$y$ plane and Onsager symmetry ensure that the electrical resistivity tensor satisfies $\rho(B) = \rho^{\mathrm{T}}(-B)$ and has non-zero components $\rho_{xx} = \rho_{yy}$ and $\rho_{xy} = -\rho_{yx}$. The tensor $\mathsf{M}$ which determines the total heat flux $U = \mathsf{M} \cdot E$ has identical symmetries [4]. The components of the thermopower $\mathsf{S}$ evaluated in the field $B$ are then given by [4,7]

$$TS_{xx} = \rho_{xx} M_{xx} - \rho_{yx} M_{yx} \tag{1a}$$

$$TS_{yx} = \rho_{yx} M_{xx} + \rho_{xx} M_{yx}. \tag{1b}$$

By solving the phonon Boltzmann equation, Lyo [2] and Fromhold *et al* [4,7] have obtained the tensor $\mathsf{M}^{\mathrm{g}}$ describing the phonon heat flux in GaAs/(AlGa)As heterostructures. This calculation assumes that the 2DEG is coupled to bulk phonons and that the electric field $E = (E,0,0)$ is established adiabatically in the presence of a quantizing magnetic field $B$. We ignore phonon reflections at the Si–SiO$_2$ interface because they are only in the order of 15% (Ezawa *et al* [8], Shinba and Nakamura [9]).

The electron–bulk phonon scattering rates in the phonon Boltzmann equation are calculated from the Fermi golden rule using fully magnetoquantized eigenstates for the 2DEG [4]. The occupancies of these states follow from the adiabatic switching of the in-plane electric field $E$. Non-electronic scattering processes are included within the relaxation-time approximation.

We have adapted this model to Si MOSFETs by using appropriate material parameters and electron–phonon scattering potentials [12]. Valley degeneracy and anisotropy of the conduction-band effective mass are also introduced. The single-subband dielectric function [13] used in the GaAs/(AlGa)As calculations is inaccurate for Si because the Landau levels are less well defined [6]. Thomas–Fermi screening is therefore preferred.

We find that the phonon drag contributions to the M tensor components are

$$M^{\mathrm{g}}_{xx} = 0 \tag{2a}$$

$$M_{yx}^{g} = -(2l^2 e/k_B T A) \sum_{q,s} \tau_{qs} \hbar\omega_{qs} v_s q_y^2 \Gamma(qs)/q \tag{2b}$$

where $A$ is the cross-sectional area of the MOSFET, $l = (\hbar/Be)^{1/2}$ is the magnetic length, $\omega_{qs}$ is the angular frequency of phonons with polarization $s$ and wavevector $q$, $\tau_{qs}$ is the relaxation time of such phonons due to non-electronic scattering processes, and $v_s = \omega_{qs}/|q| = \omega_{qs}/q$ is the group velocity of type $s$ phonons which are assumed to be non-dispersive.

In equation (2*b*)

$$\Gamma(qs) = N_{qs}^0 G \sum_{n,n'} I_{nn'}(\hbar\omega_{qs}) C_{nn'}(qs) \tag{3}$$

is the total electronic scattering rate due to type $s$ phonons with wavevector $q$. This scattering rate is proportional to the equilibrium phonon distribution function

$$N_{qs}^0 = [\exp(\hbar\omega_{qs}/k_B T) - 1]^{-1}$$

and the degeneracy of each Landau level $G = (Ag_v/2\pi l^2)$ including the valley degeneracy $g_v = 2$.

The overlap integrals

$$I_{nn'}(\hbar\omega_{qs}) = \int \mathrm{d}E\, p(E - E_n) p(E + \hbar\omega_{qs} - E_{n'}) f^0(E)[1 - f^0(E + \hbar\omega_{qs})] \tag{4}$$

depend on the Gaussian line shape

$$p(x) = (2\pi)^{-1/2} \gamma^{-1} \exp(-x^2/2\gamma^2)$$

of the $n$th Landau level $E_n = (n + \frac{1}{2})\hbar\omega_c$, where the cyclotron frequency $\omega_c = Be/m_{\parallel}^*$ depends on the effective mass associated with in-plane motion. The equilibrium Fermi function

$$f^0(E) = [\exp((E - E_F)/k_B T) + 1]^{-1}$$

varies with magnetic field as the Fermi energy $E_F$ changes to maintain a constant sheet electron concentration $n_e$.

In equation (3),

$$C_{nn'}(qs) = 2\pi \Delta_z(q_z) \Delta_{nn'}(q_{\parallel}) |V_{qs}|^2/\hbar \tag{5}$$

where

$$\Delta_{nn'}(q_{\parallel}) = (n_s!/n_l!) \chi^{n_l - n_s} [L_{n_s}^{n_l - n_s}(\chi)]^2 \exp(-\chi)$$

$q_{\parallel} = (q_x^2 + q_y^2)^{1/2}$, $\chi = (q_{\parallel} l^2)/2$, $n_s$ ($n_l$) are the smallest (largest) of $n$ and $n'$, and $L_n^m(\chi)$ is the associated Laguerre polynomial. The form factor

$$\Delta_z(q_z) = [b^2/(b^2 + q_z^2)]^3 \tag{6}$$

depends on the Fang–Howard variational parameter [11]

$$b = [12m_z e^2(N_{\rm D} + \tfrac{11}{32}n_{\rm e})/\epsilon_0\epsilon_{\rm Si}\hbar^2]^{1/3}$$

where $m_z$ is the electronic mass along $\langle 100\rangle$ and $\epsilon_{\rm Si}$ is the static dielectric constant of silicon. The aerial density of ionized acceptors in the inversion layer

$$N_{\rm D} = (2N_{\rm A}E_{\rm g}\epsilon_0\epsilon_{\rm Si}/e^2)^{1/2}$$

is determined by the volume acceptor concentration $N_{\rm A}$ in the inversion layer, and the silicon band gap $E_{\rm g}$.

The form factor given in equation (6) is only of appreciable magnitude for $|q_z| \leqslant b/2$, where $b/2$ is inversely related to the width of the 2D channel in the $z$-direction [11]. Phonons with $q_z$-values in this range interact strongly with the 2DEG because momentum in the $z$-direction is conserved within the uncertainty allowed by the 2D channel width.

The Fourier components of the transverse and longitudinal acoustic deformation scattering potentials are given by

$$|V_{q\rm t}|^2 = \hbar\omega_{q\rm t}\Xi_{\rm u}q_{\|}^2q_z^2/2\epsilon^2(q_{\|})\rho v_{\rm t}^2q^4 \tag{7a}$$

and

$$|V_{q\rm l}|^2 = \hbar\omega_{q\rm l}\Xi_{\rm u}^2((q_z^2/q^2) + D)^2/(2\epsilon^2(q_{\|})\rho v_{\rm l}^2) \tag{7b}$$

where $\rho$ is the mass density of silicon, $v_{\rm t}(v_{\rm l})$ are the group velocities of the transverse (longitudinally) polarized phonons, and $D = \Xi_{\rm d}/\Xi_{\rm u}$ is the ratio of deformation potentials relating to pure dilation and pure shear [12]. Note that equation (7a) includes contributions from both transverse polarizations.

Owing to the low electron mobilities ($\mu < 1.2$ m$^2$ V$^{-1}$ s$^{-1}$) of the Si MOSFETS described in this work, the Landau level broadening $\gamma \approx 0.6\ B^{1/2}$ meV is comparable with the inter-level separation $\hbar\omega_{\rm c}$ for $B < 4$ T. The single-subband approximation [13] for the dielectric function $\epsilon(q_{\|})$ assumes that $\gamma \ll \hbar\omega_{\rm c}$ and is thus inaccurate for Si MOSFETS, giving rise to discontinuities whenever $E_{\rm F}$ is midway between adjacent Landau levels. We therefore describe static screening using the Thomas–Fermi approximation [14]

$$\epsilon(q_{\|}) = 1 + e^2F(q_{\|})D(E_{\rm F})/[\epsilon_0(\epsilon_{\rm Si} + \epsilon_{\rm Ins})q_{\|}] \tag{8}$$

where $\epsilon_{\rm Ins}$ is the dielectric constant of $SiO_2$. The form factor

$$F(q_{\|}) = (1 + \epsilon_{\rm Ins}/\epsilon_{\rm Si})(1 + q_{\|}/b)^{-3} \times [8 + 9q_{\|}/b + 3(q_{\|}/b)^2]/16 + (1 - \epsilon_{\rm Ins}/\epsilon_{\rm Si})(1 + q_{\|}/b)^{-6}/2 \tag{9}$$

accounts for the spread of the 2DEG wavefunction normal to the interface [15]. We restrict our calculations to $T < 6$ K because at higher temperatures phonons are

excited with sufficiently short wavelengths that equation (9) becomes inaccurate. In this limit a multisubband dielectric function should be used [16].

Due to the stronger screening in Si MOSFETs, the phonon drag thermopower is approximately three orders of magnitude lower than in GaAs/(AlGa)As heterojunctions [12]. Below $T = 2$ K the drag contribution is small compared with that due to electron diffusion [6]. To accurately describe the magnetothermopower at low temperatures we must therefore determine tensor components $M^{\mathrm{d}}_{xx}$ and $M^{\mathrm{d}}_{yx}$ which give the heat flux due to electron diffusion. The total heat flux is then $\boldsymbol{U} = \mathsf{M} \cdot \boldsymbol{E}$ where $\mathsf{M} = \mathsf{M}^{\mathrm{g}} + \mathsf{M}^{\mathrm{d}}$.

It follows from the definition of electron heat flux [17,18] that

$$M^{\mathrm{d}}_{xx} = \frac{1}{e}\int \frac{\partial f^0}{\partial E}(E - E_{\mathrm{F}})\sigma_{xx}(E)\,\mathrm{d}E \tag{10}$$

$$M^{\mathrm{d}}_{yx} = \frac{1}{e}\int \frac{\partial f^0}{\partial E}(E - E_{\mathrm{F}})\sigma_{yx}(E)\,\mathrm{d}E. \tag{11}$$

The energy-dependent tensors $\sigma_{xx}(E)$ and $\sigma_{yx}(E)$ determine the electrical conductivities $\sigma_{xx}(E_{\mathrm{F}})$ and $\sigma_{yx}(E_{\mathrm{F}})$ at absolute zero. Gerhardts [10] has shown using the lowest-order cumulant approximation to describe transitions between Landau states with different orbit centres that,

$$\sigma_{xx}(E) = \frac{2e^2 g_{\mathrm{v}}}{h}\sum_n (n + \tfrac{1}{2})\exp[-(E - E_n)^2/\gamma^2] \tag{12}$$

and

$$\sigma_{yx}(E) = \frac{e^2 g_{\mathrm{v}}}{h}\sum_n 1 + \mathrm{erf}[(E - E_n)/\sqrt{2}\gamma] \tag{13}$$

when a Gaussian density of states is assumed. At low $T$, magneto-oscillatory structure in $\sigma_{xx}(E)$ and $\sigma_{yx}(E)$ is expected to impose oscillations on $\mathsf{M}$ and on the thermopower tensor $\mathsf{S}$ [17,18]. For simplicity spin-splitting has been omitted from both the drag and diffusion theories.

## 3. Comparison with experiment

Figure 1 shows that at $T = 5.02$ K the theoretical $M_{yx}(B)$ curve is drag-dominated and is in reasonable quantitative agreement with experiment, in which no spin-splitting is revealed. The observed and predicted values of $|M_{yx}|$ both decrease with increasing magnetic field and contain oscillations in phase with those of $D(E_{\mathrm{F}})$. The Landau level width parameter $C = 0.6$ meV $\mathrm{T}^{-1/2}$ is close to the value $\approx 0.4$ meV $\mathrm{T}^{-1/2}$ given by the self-consistent Born approximation [6].

Comparison of figures 1 and 2 shows that for $B > 3$ T experimental values of $|M_{xx}|$ are generally less than 25% of the corresponding $|M_{yx}|$ values. The observed $M_{xx}$-values are negative for $B \leqslant 4$ T and oscillate about zero for higher fields.

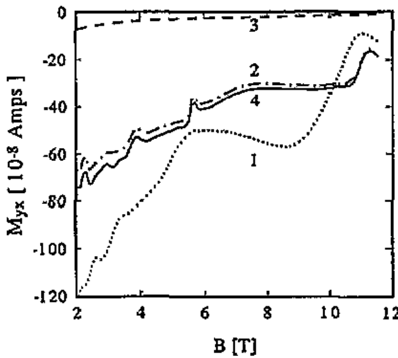


**Figure 1.** Comparison of theoretical and experimental values of $M_{yx}$ for a Si MOSFET with $n_e = 10.7 \times 10^{15}$ m$^{-2}$ at $T = 5.02$ K. Curve 1: experimental values. Curve 2: theoretical phonon drag contribution. Curve 3: theoretical electronic diffusion contribution. Curve 4: sum of theoretical drag and diffusion values. For curves 2, 3 and 4, $\gamma = 0.6\ B^{1/2}$ meV. For curves 2 and 4, $\lambda_p = 1.13$ mm.

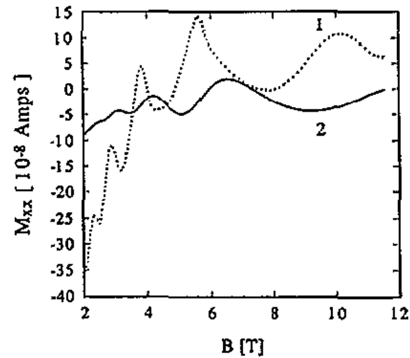


**Figure 2.** Comparison of experimental values of $M_{xx}$ (curve 1) and the theoretical diffusion contribution (curve 2) for a Si MOSFET with $n_e = 10.7 \times 10^{15}$ m$^{-2}$ at $T = 5.02$ K. For curve 2, $\gamma = 0.6\ B^{1/2}$ meV. Note that the predicted drag contribution is zero.

By contrast, measurements on GaAs/(AlGa)As heterojunctions reveal positive $M_{xx}$ values up to 60% of those of $|M_{yx}|$ [4].

The predicted diffusion contribution to $M_{xx}$ shown in figure 2 is of similar magnitude to the experimental value, indicating that the drag contribution is less important than for $M_{yx}$. However, to accurately model the phase and magnitude of the $M_{xx}$ oscillations, the drag theory must be extended to give a non-zero contribution $M^{\rm g}_{xx}$. Ways in which this may be done are discussed by Fromhold *et al* [4].

The curves labelled 1 in figures 3 and 4 show experimental $-S_{xx}$ and $S_{yx}$ data for a Si MOSFET at $T = 5.02$ K. We anticipate that setting the drag contribution $M^{\rm g}_{xx} = 0$ in equation (1) will compromise the accuracy of our theoretical $-S_{xx}$ and $S_{yx}$ values. For comparison with experiment figures 3 and 4 therefore show $-S_{xx}$ and $S_{yx}$ curves calculated from theoretical $M_{yx}$ values together with experimental data for $\rho_{xx}$ and $\rho_{yx}$, and either using experimental values of $M_{xx}$ (curve 2) or setting $M_{xx} = M^{\rm d}_{xx}$ with $M^{\rm g}_{xx} = 0$ (curve 3). Both theoretical S($\boldsymbol{B}$) curves are drag-dominated. Maxima in the absolute values of $-S_{xx}$ coincide with those in $S_{yx}$ and $D(E_{\rm F})$, when the number of electronic states participating in the electron–phonon scattering processes is highest and the phonon distribution deviates furthest from equilibrium.

The effect of setting $M^{\rm g}_{xx} = 0$ in equation (1) can be seen by comparing figures 3 and 4. The $-S_{xx}$ values predicted within this approximation do not differ significantly from those obtained using empirical $M_{xx}$ data, whereas the agreement between the measured and calculated $S_{yx}$ curves is significantly reduced. In particular the oscillatory structure in $S_{yx}$ is over-emphasized and no longer in phase with experiment.

That $M^{\rm g}_{xx}$ is less influential to $S_{xx}$ can be understood from equation (1). Provided there is little disorder in the system $|M_{xx}| \ll |M_{yx}|$, as shown in figures 1 and 2,

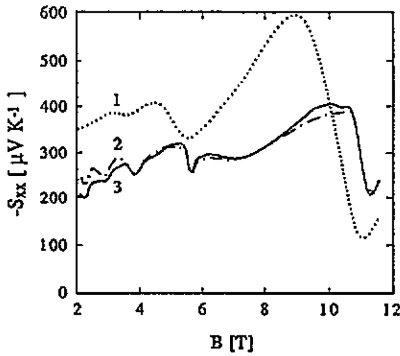


**Figure 3.** Comparison of theoretical and experimental values of $-S_{xx}$ for a Si MOSFET with $n_e = 10.7 \times 10^{15}$ m$^{-2}$ at $T = 5.02$ K. Curve 1: experimental values. Curve 2: sum of theoretical diffusion contribution and drag contribution calculated using empirical $M_{xx}$ data. Curve 3: sum of theoretical diffusion and drag contributions taking $M^{g}_{xx} = 0$. For curves 2 and 3, $\gamma = 0.6\ B^{1/2}$ meV and $\lambda_p = 1.13$ mm.

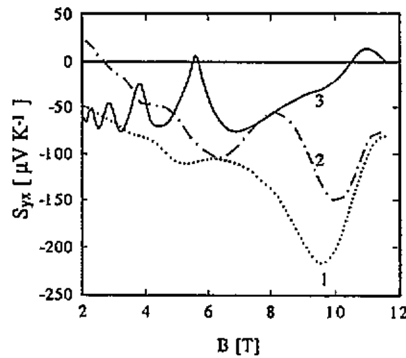


**Figure 4.** Comparison of theoretical and experimental values of $S_{yx}$ for a Si MOSFET with $n_e = 10.7 \times 10^{15}$ m$^{-2}$ at $T = 5.02$ K. Curve 1: experimental values. Curve 2: sum of theoretical diffusion contribution and drag contribution calculated using empirical $M_{xx}$ data. Curve 3: sum of theoretical diffusion and drag contributions taking $M^{g}_{xx} = 0$. For curves 2 and 3, $\gamma = 0.6\ B^{1/2}$ meV and $\lambda_p = 1.13$ mm.

and $|\rho_{xx}| \ll |\rho_{yx}|$. The second term on the right-hand side (RHS) of equation (1*a*) therefore dominates the first and the field-dependence of $-S_{xx}$ mainly follows the behaviour of $M_{yx}$.

By contrast, both terms on the RHS of equation (1*b*) are of comparable magnitude. The diffusion contribution to $M_{xx}$ does not adequately account for the observed variation so that non-zero $M^{g}_{xx}$ values must be included in equation (1*b*) in order to reproduce the experimental $S_{yx}$ data.

Calculations of $S_{yx}$ in GaAs/(AlGa)As heterostructures also depend critically on $M^{g}_{xx}$ [4]. Previous studies of such structures demonstrated excellent agreement between experimental and theoretical $-S_{xx}$ values [2] but did not consider $S_{yx}$ and so failed to reveal the crucial importance of $M^{g}_{xx}$ to this off-diagonal component.

Calculations of $S_{yx}$ in Si MOSFETs at $T = 2.99$ K also reveal a dominant drag contribution and are in reasonable agreement with experiment even taking $M^{g}_{xx}$ to be zero [6]. We stress that good agreement within this approximation is probably fortuitous.

Figures 5 and 6 show experimental $-S_{xx}$ and $S_{yx}$ data for a Si MOSFET at $T = 1.47$ K. At this temperature the thermopower curves are calculated using $M_{xx} = M^{d}_{xx}$, with $\rho_{xx} = 0$ and $\rho_{yx} = -B/en_e$ following Lyo [2]. For temperatures $T < 2$ K, the drag contribution to $-S_{xx}$ is suppressed and small compared with the diffusion component which oscillates in phase with $D(E_F)$. The predicted diffusion contribution to $-S_{xx}$ is of the same order of magnitude as the data. However, the oscillatory amplitudes are underestimated in the theory which does not reproduce the spin splitting of the $n = 2$ Landau level observed for $B \approx 7$ T.

When finite $\rho_{xx}$ values, obtained using the lowest-order cumulant approximation for inter-Landau state scattering [10], were used to calculate $-S_{xx}$ for a similar MOSFET at $T = 1.47$ K, the observed oscillatory amplitudes were well accounted for. We therefore suggest that *at low temperatures* the first term on the RHS of equation

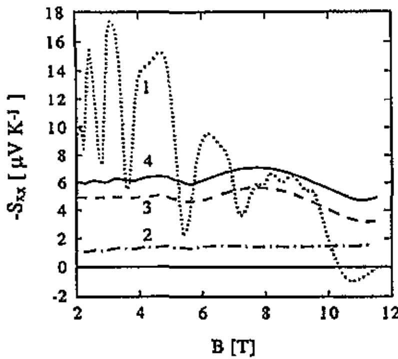


**Figure 5.** Comparison of theoretical and experimental values of $-S_{xx}$ for a Si MOSFET with $n_e = 10.7 \times 10^{15}$ m$^{-2}$ at $T = 1.47$ K. Curve 1: experimental values. Curve 2: theoretical phonon drag contribution taking $M^{g}_{xx} = 0$. Curve 3: theoretical electronic diffusion contribution. Curve 4: sum of predicted drag and diffusion values. For curves 2, 3 and 4, $\rho_{xx} = 0$, $\rho_{yx} = -B/en_e$, and $\gamma = 0.6\ B^{1/2}$ meV. For curves 2 and 4, $\lambda_p = 1.19$ mm.

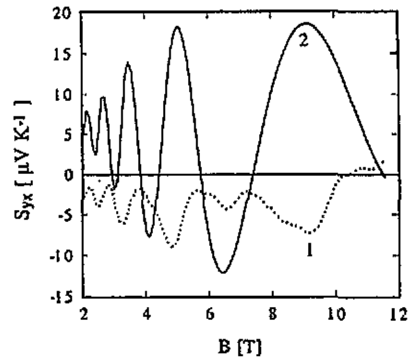


**Figure 6.** Comparison of experimental values of $S_{yx}$ (curve 1) with the theoretical diffusion contribution (curve 2) for a Si MOSFET with $n_e = 10.7 \times 10^{15}$ m$^{-2}$ at $T = 1.47$ K. For curve 2, $\rho_{xx} = 0$, $\rho_{yx} = -B/en_e$, $\gamma = 0.6\ B^{1/2}$ meV, and $\lambda_p = 1.19$ mm. Note that the predicted drag contribution vanishes since both $\rho_{xx}$ and $M^{g}_{xx}$ are taken to be zero.

(1$a$) dominates the behaviour of $S_{xx}$. The second term is more important at higher temperatures [4].

When $M^{g}_{xx}$ and $\rho_{xx}$ are both zero the off-diagonal thermopower component (1$b$) reduces to $S_{yx} = M^{d}_{xx}\rho_{yx}/T$ and contains no drag contribution. The $S_{yx}$-values predicted within these approximations are in poor agreement with experiment as shown in figure 6. In particular the oscillatory structure is over-emphasized and out of phase with experiment.

Using finite theoretical values of $\rho_{xx}$ [10] somewhat improves the agreement with experiment [6]. However, the accuracy of the theoretical $S_{yx}$ curves is primarily limited by the energy-dependent conductivity tensors (12) and (13) which are single-subband expressions [13] and thus do not take into account the considerable overlap between adjacent Landau levels at low magnetic fields.

## 4. Conclusions

We have calculated the heat transport and thermopower tensors **M** and **S** of a 2DEG in a Si MOSFET as a function of magnetic field $B \| \langle 100 \rangle$ normal to the plane of the 2DEG.

At $T = 5.02$ K both **M** and **S** are dominated by the heat flux which originates as the phonon distribution is dragged from equilibrium by electron–phonon scattering. Assuming the 2DEG interacts with 3D Si phonons and that the in-plane electric field is established adiabatically, solution of the phonon Boltzmann equation predicts $M^{g}_{xx} = 0$ and $M^{g}_{yx} < 0$. Thermoelectrical $-S_{xx}(B)$ curves obtained using these predicted values of **M** together with experimental values for $\rho$ are in good agreement with experiment. Screening of the electron–phonon interaction is crucial and reduces

the peak value of $-S_{xx}$ by three orders of magnitude. The predicted $S_{yx}$ curves depend critically on $M^{g}_{xx}$ and are in poor qualitative agreement with experiment when $M^{g}_{xx} = 0$. However, when experimental values of $M^{g}_{xx}$ are substituted good agreement is obtained with experiment for both the $-S_{xx}$ *and* $S_{yx}$ curves.

At temperatures $T < 2$ K, the thermopower components are dominated by electron diffusion. The predicted diffusion contributions to the thermopower tensor **S** are of the correct order of magnitude, although the oscillatory structure is underestimated in $-S_{xx}$ and overemphasized in $S_{yx}$.

In order to adequately reproduce the experimental $S_{yx}$ curves in the drag-dominated regime $T > 2$ K without recourse to experimental data, further theoretical work is required to obtain finite values of $M^{g}_{xx}$ and to calculate the resistivity tensor $\rho$ including quantum Hall effects.

## Acknowledgments

The authors would like to thank the Science and Engineering Research Council for financial support.

## Appendix. Parameter values

The numerical values of the silicon parameters used in the calculation are $\epsilon_{\mathrm{Si}} = 11.5$, $\epsilon_{\mathrm{Ins}} = 3.9$, $m_z^* = 0.916m_0$, $m_{\parallel}^* = 0.19m_0$, where $m_0$ is the free electron mass, $v_l = 8.831\times10^3$ m s$^{-1}$, $v_t = 5.281\times10^3$ m s$^{-1}$, $\rho = 2.39\times10^3$ kg m$^{-3}$, $E_g = 1.12$ eV, $\Xi_u = 9$ eV, $\Xi_d = -6$ eV, $N_A = 1.5\times10^{19}$ m$^{-3}$. The phonon relaxation time $\tau_{qs} = \lambda_p/v_s$ where $\lambda_p$ is a phonon mean free path for non-electronic scattering processes. This is measured as a function of $T$ for all the samples we discuss, along with the sheet electron density $n_e$.

## References


[1] Kubakaddi S, Butcher P N and Mulimani B G 1989 *Phys. Rev.* B **40** 1377

[2] Lyo S K 1989 *Phys. Rev.* B **40** 6458

[3] Cantrell D G and Butcher P N 1987 *J. Phys. C: Solid State Phys.* **20** 1985, 1993

[4] Fromhold T M, Butcher P N, Qin G, Mulimani B G, Oxley J P and Gallagher B L 1993 *Phys. Rev.* B submitted

[5] Gallagher B L, Oxley J P, Galloway T, Smith M J and Butcher P N 1990 *J. Phys.: Condens. Matter* **2** 755

[6] Oxley J P, Gallagher B L, Galloway T, Butcher P N, Fromhold T M, Mulimani B G and Karavolas V 1990 *Proc. 20th Int. Conf. on the Physics of Semiconductors* ed E M Anastassakis and J D Joannopoulos (Singapore: World Scientific) pp 853–6

[7] Fromhold T M, Butcher P N, Qin G, Mulimani B G, Oxley J P and Gallagher B L 1992 *Surf. Sci.* **263** 183

[8] Ezawa H, Kawaji S and Nakamura K 1974 *Japan. J. Appl. Phys.* **13** 126

[9] Shinba Y and Nakamura K 1981 *J. Phys. Soc. Japan* **50** 114

[10] Gerhardts R 1975 *Z. Phys.* B **21** 285

[11] Fang F and Howard W E 1966 *Phys. Rev. Lett.* **16** 797

[12] Smith M J and Butcher P N 1989 *J. Phys.: Condens. Matter* **1** 1261

[13] Murayama Y and Ando T 1987 *Phys. Rev.* B 35 2252
[14] Tamura S and Kitagawa H 1989 *Phys. Rev.* B 40 8485
[15] Ando T, Fowler A B and Stern F 1982 *Rev. Mod. Phys.* **54** 454
[16] Ando T and Uemura Y 1974 *J. Phys. Soc. Japan* **37** 1044
[17] Jonson M and Girvin S M 1984 *Phys. Rev.* B 29 1939
[18] Oji H 1984 *J. Phys. C: Solid State Phys.* 17 3059